Electronic Supplementary Information

Ab initio study of nickel-catalyzed transformation of amorphous carbon into graphene in rapid thermal processing

Shuang Chen,[ab] Wei Xiong,[c] Yun Shen Zhou,[c] Yong Feng Lu[c] and Xiao Cheng Zeng*[a]

[a]Department of Chemistry, University of Nebraska–Lincoln, Lincoln, Nebraska 68588, United States

[b]Kuang Yaming Honors School, Nanjing University, Nanjing, Jiangsu 210023, China

[c]Department of Electrical and Computer Engineering, University of Nebraska-Lincoln, Lincoln, Nebraska 68588, United States

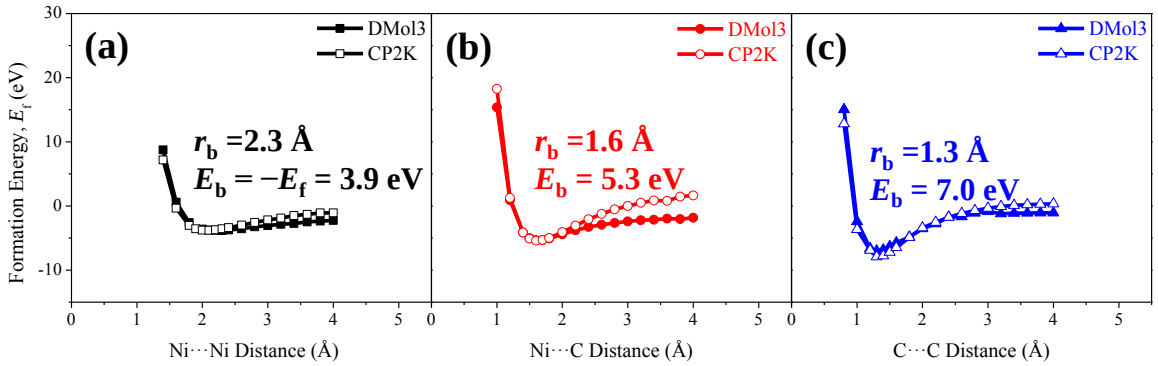

Fig. S1 Formation energies of Ni···Ni, Ni···C, and C···C as a function of interatomic distance computed using the spin-polarized DFT PBE-D2 method with the double numerical basis set plus polarization (DNP) (implemented in DMol^3 7.0), and using the PBE-D3 and GWP methods (implemented in CP2K). The minimum of the formation energy curve corresponds to bond distance (r_b) and bond energy (E_b) between two bonding atoms. Based on the formation energy curves, the interaction strength in Ni-C system can be estimated to follow this general trend, Ni-Ni < Ni-C < C-C, consistent with the cohesive energy trend of Ni < C (see Kittel C. *Introduction to Solid State Physics*; John Wiley & Sons: New York, 1996).

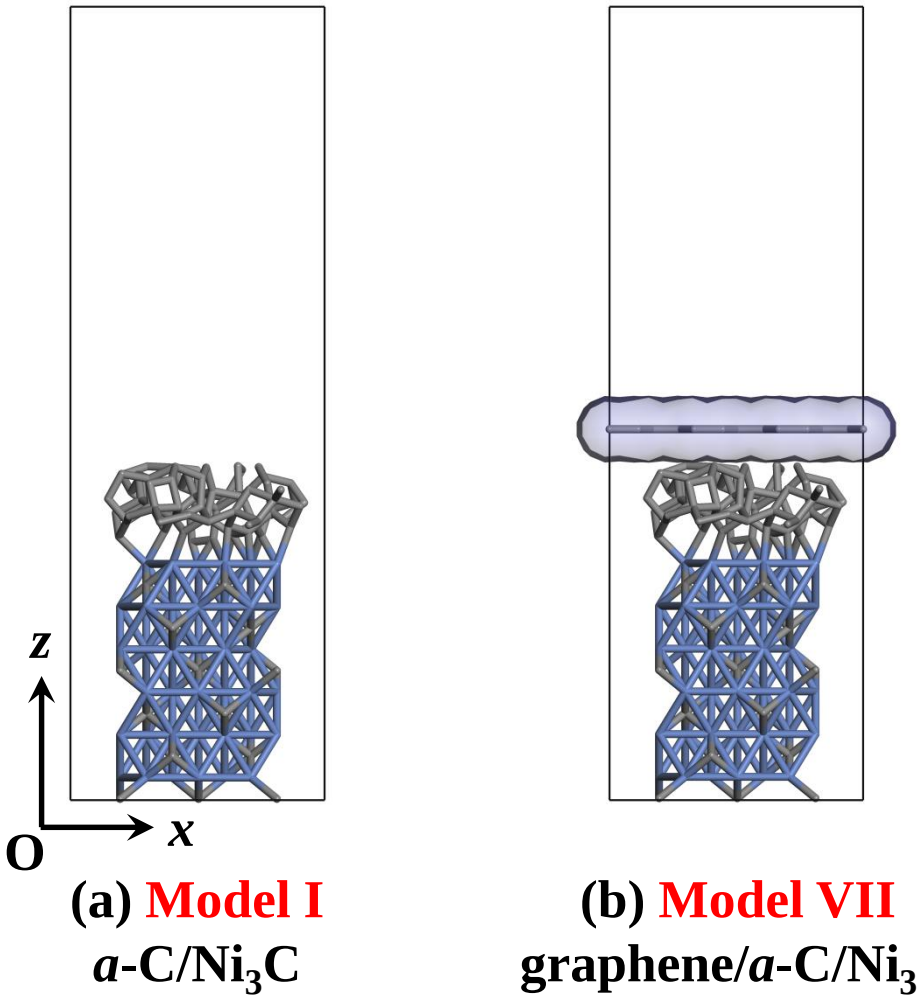

Fig. S2 Initial configurations of (a) Model I *a*-C/Ni_3C and (b) Model VII graphene/*a*-C/Ni_3C. The Ni and C atoms are shown in blue and grey, respectively, and the perfect first graphene layer is also highlighted with purple vdW surface. Both slab models are viewed along the *y* axis to show the vacuum layer.

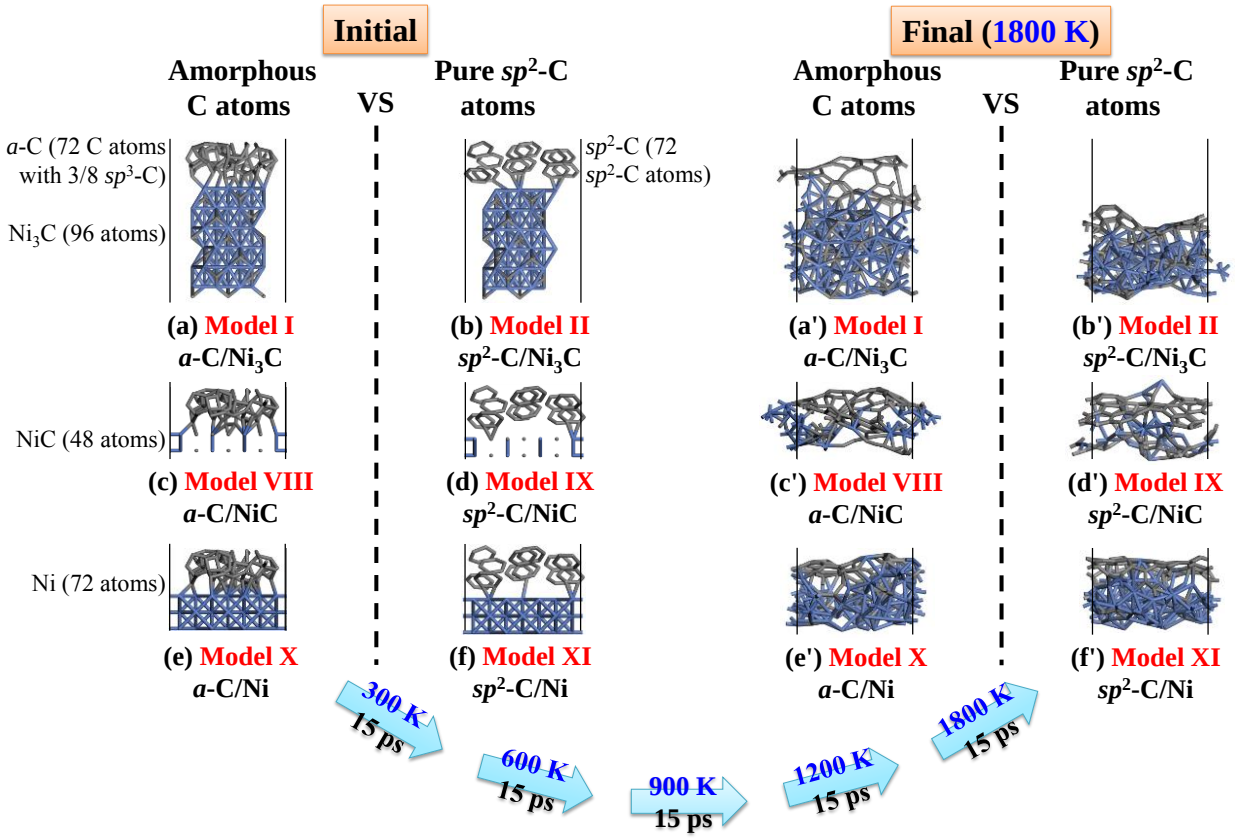

Fig. S3 Initial (a-f) and final configurations of (a'-f') of Model I *a*-C/Ni_3C, Model II sp^2-C/Ni_3C, Model VIII *a*-C/NiC, Model IX sp^2-C/NiC, Model X *a*-C/Ni, and Model XI sp^2-C/Ni based on stepwise temperature increase from 300 K, 600 K, 900 K, 1200 K, to 1800 K every 15 ps in AIMD simulations. The Ni and C atoms are shown in blue and grey, respectively. The number of C atom or Ni atom in each model is also highlighted in insets. All the slab models are viewed along the surface *y* axis, and the vacuum layer along the *z* axis for each model is cut to highlight reactive solid layers.

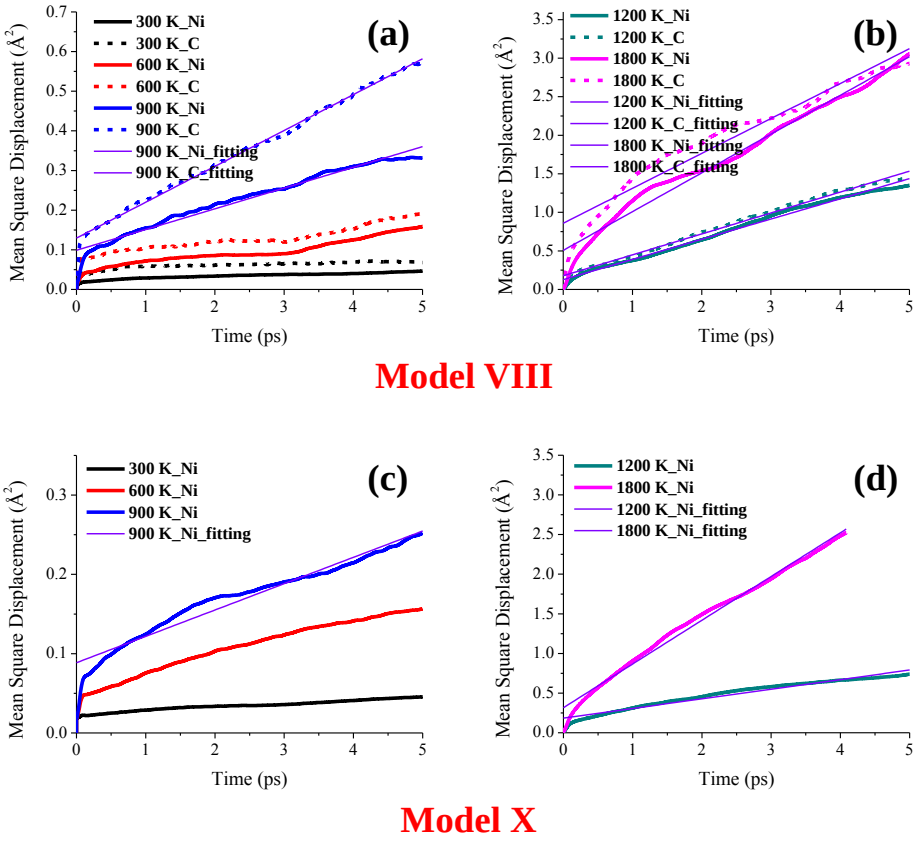

Fig. S4 Variations of mean square displacement (MSD) with time for Ni (solid lines) and C (dashed lines) atoms in NiC layer of Model VIII at (a) 300 K, 600 K, and 900 K and (b) 1200 K and 1800 K, and for Ni atoms in Ni layer of Model X at (c) 300 K, 600 K, and 900 K and (d) 1200 K and 1800 K based on the AIMD simulations. The corresponding linear fitting of the MSD-time curves are in violet.

Table S1 Computed self-diffusion coefficients, D (unit: cm^2/s), of Ni or C atoms in Ni_3C layer of Model I, NiC layer of Model VIII, and Ni layer of Model X at different temperatures (stepwise increase every 15 ps) through linear fitting of MSD-time curves shown in Fig. 2 of the main text and Fig. S4, respectively, on basis of AIMD simulations.

	900 K	1200 K	1800 K
		Ni_3C layer of Model I	
Ni	3.3×10^{-7}	6.4×10^{-7}	3.7×10^{-6}
C	4.8×10^{-7}	1.6×10^{-6}	8.6×10^{-6}
		NiC layer of Model VIII	
Ni	8.7×10^{-7}	4.4×10^{-6}	8.4×10^{-6}
C	1.5×10^{-6}	4.5×10^{-6}	7.5×10^{-6}
		Ni layer of Model X	
Ni	5.5×10^{-7}	2.0×10^{-6}	9.2×10^{-6}

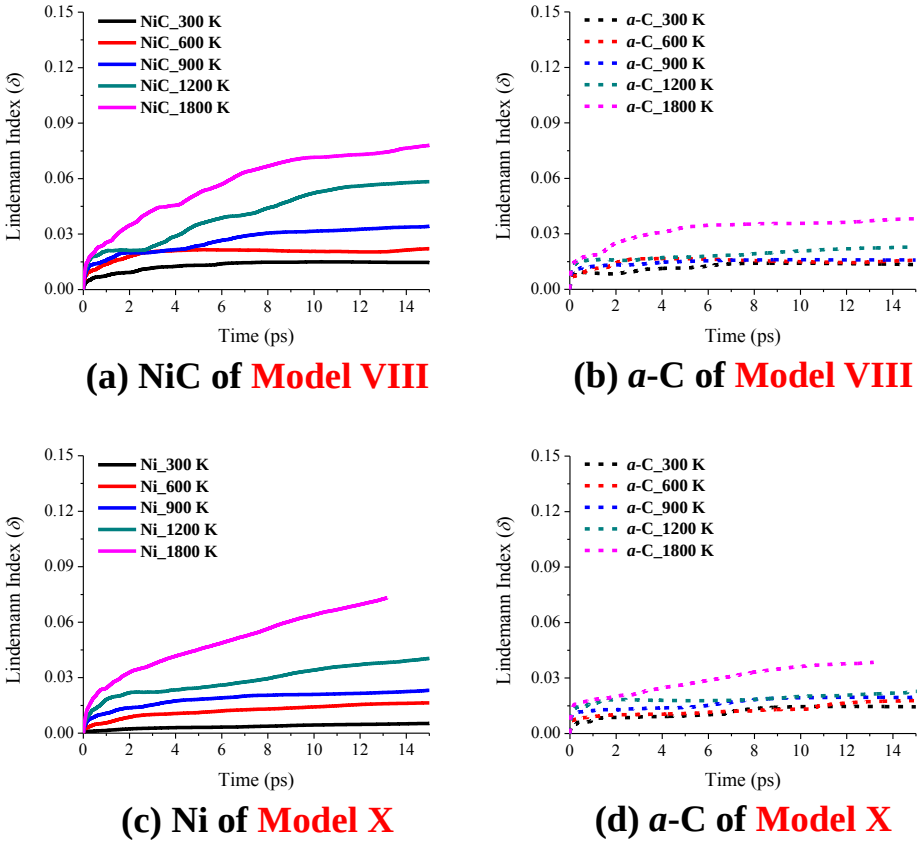

Fig. S5 Lindemann index (δ) of (a) NiC layer and (b) *a*-C layer in Model VIII and of (c) Ni layer and (d) *a*-C layer in Model X, estimated from the 15-ps AIMD simulations with temperature increase from 300 K, 600 K, 900 K, 1200 K, to 1800 K.